JACS
JOURNAL OF THE AMERICAN CHEMICAL SOCIETY
pubs.acs.org/JACS
Article

# ATP-Responsive Liposomes via Screening of Lipid Switches Designed to Undergo Conformational Changes upon Binding Phosphorylated Metabolites

Jinchao Lou, Jennifer A. Schuster, Francisco N. Barrera, and Michael D. Best*

Cite This: J. Am. Chem. Soc. 2022, 144, 3746−3756
Read Online



**ABSTRACT:** Liposomal delivery vehicles can dramatically enhance drug transport. However, their clinical application requires enhanced control over content release at diseased sites. For this reason, triggered release strategies have been explored, although a limited toolbox of stimuli has thus far been developed. Here, we report a novel strategy for stimuli-responsive liposomes that release encapsulated contents in the presence of phosphorylated small molecules. Our formulation efforts culminated in selective cargo release driven by ATP, a universal energy source that is upregulated in diseases such as cancer. Specifically, we developed lipid switches **1a−b** bearing two ZnDPA units designed to undergo substantial conformational changes upon ATP binding, thereby disrupting membrane packing and triggering the release of encapsulated contents. Dye leakage assays using the hydrophobic dye Nile red validated that ATP-driven release was selective over 11 similar phosphorylated metabolites, and release of the hydrophilic dye calcein was also achieved. Multiple alternative lipid switch structures were synthesized and studied (**1c−d** and **2**), which provided insights into the structural features that render **1a−b** selective toward ATP-driven release. Importantly, analysis of cellular delivery using fluorescence microscopy in conjunction with pharmacological ATP manipulation showed that liposome delivery was specific, as it increased upon intracellular ATP accumulation, and was inhibited by ATP downregulation. Our new approach shows strong prospects for enhancing the selectivity of release and payload delivery to diseased cells driven by metabolites such as ATP, providing an exciting new paradigm for controlled release.

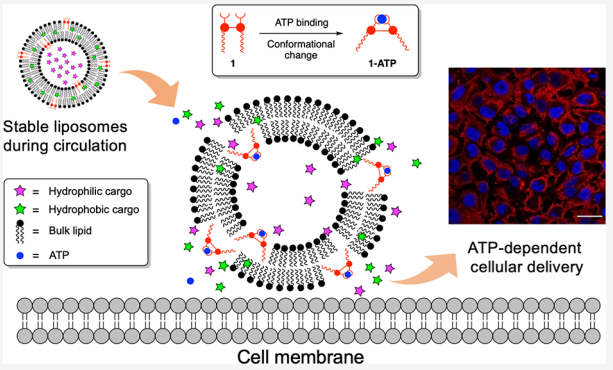


## INTRODUCTION

Liposomal nanoparticles are effective molecular cargo containers for the encapsulation and delivery of a wide range of therapeutic agents.[1] Indeed, several liposome formulations have been approved for clinical applications by the US Food and Drug Administration (FDA) and additional constructs are undergoing clinical trials.[2,3] These applications have resulted from key advancements in liposome delivery properties, including the decoration of liposome surfaces with poly (ethylene glycol) (PEG) to dramatically enhance circulation time,[4] additives such as cationic lipids or lipopeptides to advance infiltration of cells,[5] and targeting moieties such as antibodies and peptides to enhance selective delivery to diseased cells.[6]

However, a key aspect of liposomal drug delivery that remains difficult to control is the timing and location of encapsulated cargo release. This provides an important opportunity to maximize payload delivery, control subcellular drug localization, and enhance selectivity toward diseased cells. As a result, the development of stimuli-responsive liposomes is a vigorous area of research in which a number of stimuli have been explored for controlling cargo release.[7,8] These are categorized as passive release (internal stimuli intrinsic to diseased cells, i.e., pH,[9,10] redox,[11−13] and enzyme expression[14,15]) or active release (external stimuli, i.e., light,[16,17] heat,[18,19] and ultrasound[20]). Despite these efforts, liposome-triggered release is yet to be incorporated into clinical liposome applications due to multiple challenges. Internal stimuli commonly suffer from minimal differences between diseased and healthy cells. For example, while the extracellular environment of cancer cells is acidic and pH-responsive liposomes have thus been heavily studied, there is a narrow window for triggered release (pH 6.5−6.7 for cancer cells compared to pH 7.2−7.4 for healthy cells).[21] For active release, it is challenging to deliver stimuli in a nondestructive

Received: January 6, 2022
Published: February 16, 2022

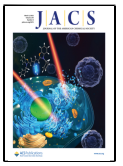

manner. For example, the UV light needed for photoresponsive liposomes exhibits ineffective tissue penetration and is toxic to healthy tissue.[22]

The current work pertains to a new paradigm in which small molecule metabolites can be harnessed to trigger content release from liposomes by directly binding lipid switches and perturbing membrane properties. This is because overly abundant metabolites are commonly associated with diseased cells, offering a promising strategy for selective drug delivery. A challenge in this endeavor entails the extension of molecular recognition principles in a manner that will modulate liposome self-assembly properties. We previously developed similar approaches by engineering calcium- and zinc-responsive liposome platforms.[23,24] Here, lipid switches were designed such that calcium or zinc binding induced a conformational change that was effective for modulating membrane properties and driving cargo release. While ions provided strategic targets for proof-of-concept due to the existence of known sensors that exhibit high affinity and selectivity, small molecules present significant challenges due to the dearth of clinically relevant host structures and the presence of multiple functional groups with varying three-dimensional presentation.

Here, we report direct liposome-triggered release driven by phosphorylated small molecules, which culminated in selective adenosine triphosphate (ATP)-responsive liposomes. Phosphorylated metabolites are of particular interest since the introduction of phosphate groups into biomolecules is a critical means for regulating biological function.[25,26] ATP is an excellent target for metabolite-driven release due to its high concentration and critical roles in biological systems. It is a universal energy source that controls vital biological processes including signaling,[27,28] energy transduction,[29,30] regulation of cellular metabolism,[31,32] and DNA replication.[33,34] While ATP exhibits low concentrations in the extracellular space of healthy tissues (0.01−0.1 mM),[35] increases in ATP concentration up to the high mM range are associated with tumors resulting from conditions including inflammation, hypoxia, and mechanical stresses.[36−38] Therefore, in the development of platforms for drug release driven by the binding of small molecules, ATP provides an exciting prospective stimulus for liposome triggered release. The concept of ATP responsiveness has been validated using other delivery carriers featuring different mechanisms.[39−43] In a rare case employing liposomes, Gu and co-workers[44] reported a co-delivery system employing a cell-penetrating peptide fusogenic shell and a core DNA−protein conjugate that is activated by supplemental liposome-encapsulated ATP. While this elegant work confirmed that ATP-mediated delivery can enhance anti-cancer therapeutic efficacy, a direct approach in which liposome membrane properties are modulated via incorporated lipid switches as presented herein provides an efficient strategy that does not require multiple protein and DNA additives to trigger cargo escape.

## RESULTS AND DISCUSSION

### Design and Synthesis of ATP-Responsive Liposomes.

The development of stimuli-responsive liposomes presents design challenges pertaining to the conditions invoked to perturb membranes for cargo release. Prior work has commonly employed modifications to naturally existing non-bilayer lipids[45] such as dioleoylphosphatidylethanolamine (DOPE) to alter lipid packing.[46] However, this system offers only subtle changes to membrane packing. Therefore, high percentages of stimuli-responsive lipids are typically required in liposome formulations, which are not amenable to clinical applications due to instability issues. To overcome this obstacle, rationally designed synthetic lipid switches have recently emerged as a more effective means to trigger content release. By engineering the lipid structure and through the power of chemical synthesis, more significant structural changes that perturb membrane properties can be designed to occur upon stimuli addition.[47,48] A pioneering example of this approach was reported by Leblond and co-workers,[49,50] where they developed a pH-responsive lipid switch for which acidification facilitated hydrogen bond formation that induced a conformational change in the lipid structure, leading to the release of entrapped cargo. This work inspired our efforts to develop calcium- and zinc-responsive liposomes as well as the current work.

To develop liposomes that respond to phosphorylated small molecules, we initially designed artificial lipid switches of type **1** containing zinc(II) dipicolylamine (ZnDPA) groups, which culminated in the discovery of ATP-responsive properties. ZnDPA moieties were included since they effectively bind phosphorylated functional groups with high affinity.[51−53] Building upon the success of our previous calcium-responsive lipid switch, we mounted two ZnDPA groups onto rigid scaffolds (of type **1**; Scheme 1A) so that the resulting lipid can thus rest comfortably within liposomal membranes in the unbound form. Binding to phosphorylated small molecules was designed to induce a conformational change that produces lipid products exhibiting conical shapes. This was envisaged to disrupt membrane packing and trigger the release of

**Scheme 1. Design for Phosphorylated Metabolite-Responsive Liposomes**[a]

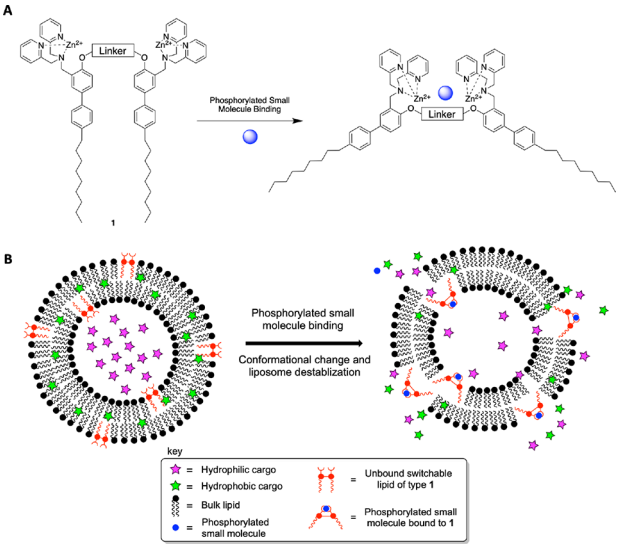


[a](A) General structures of responsive lipids of type **1** bearing two ZnDPA units. These lipids are designed to adopt a cylindrical structure in the membrane prior to guest treatment. Chelation of an appropriate phosphorylated molecule is expected to lead to an increased cone angle and non-bilayer properties. (B) Cartoon depiction of liposome release driven by phosphorylated metabolite addition. The conformational change upon guest molecule binding is expected to disrupt membrane integrity and trigger encapsulated cargo release.



https://doi.org/10.1021/jacs.2c00191
J. Am. Chem. Soc. 2022, 144, 3746−3756

**Scheme 2. General Synthetic Route to Bis-ZnDPA Lipid Structures 1a−b**[a]

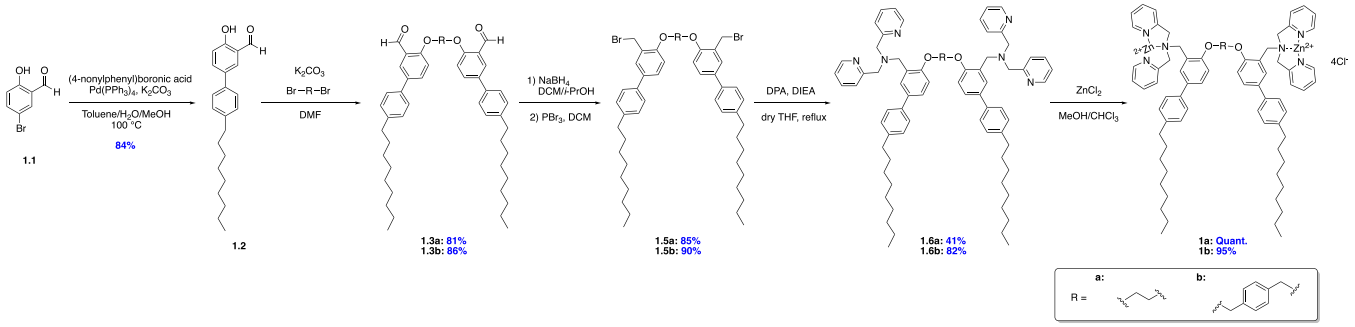


[a]Compound **1.1** was coupled with (4-nonylphenyl)boronic acid to produce **1.2** followed by dimerization using dibromoethane to **1.3a** or *p*-xylene dibromide to **1.3b**, aldehyde reduction and bromination to **1.5a-b**, introduction of the DPA units of **1.6a-b**, and finally, zinc chelation to generate **1a−b**.

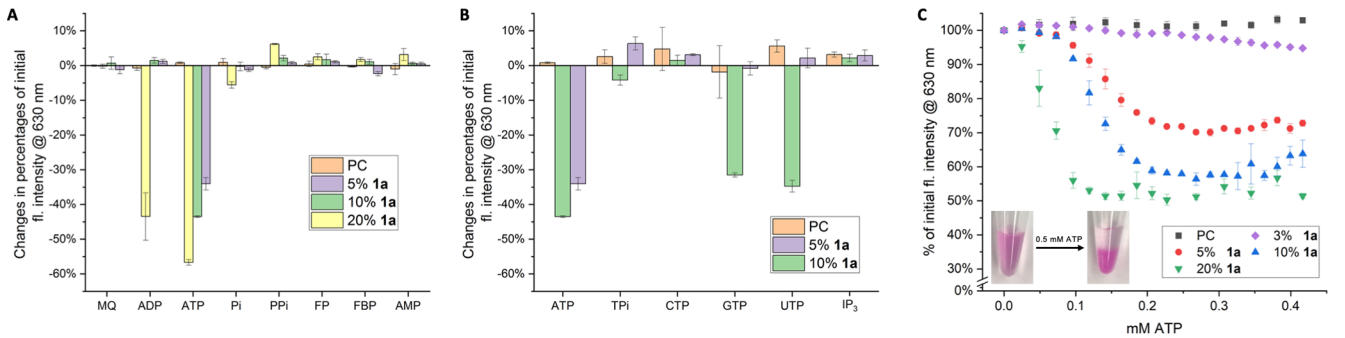


**Figure 1.** NR release results from liposomes containing lipid switch **1a**. (A) Selectivity screens of PC/**1a** liposomes toward different phosphorylated small molecules or simply Milli-Q water (MQ). While liposomes containing 20% **1a** released NR upon both ADP and ATP addition, decreasing incorporation to 10 and 5% resulted in liposomes that only responded to ATP. (B) Selectivity of **1a** liposomes toward different triphosphates. Liposomes with 10% **1a** responded to both GTP and UTP, while those with 5% **1a** liposomes did not exhibit release for any nucleotide triphosphates other than ATP. (C) ATP titration curves for **1a** liposomes showing dose-dependent release depending on the percentage of **1a**. Error bars denote standard errors from at least three independent studies. Inset: images of NR-encapsulated liposome solutions before and after ATP treatment showing pink precipitate formation.

encapsulated cargo by amplifying the properties of naturally existing non-bilayer lipids (Scheme 1B).[45]

Since it is difficult to predict the exact host design and cavity size that would fit metabolite targets, we designed lipid structures bearing linkers of different lengths and rigidities between the two ZnDPA groups. Initial switches included a short ethylene linker (**1a**) and a slightly longer aromatic *p*-xylene linker (**1b**). Further variants designed to probe structural effects on release will be subsequently described. The synthetic route to initial compounds **1a** and **1b** is shown in Scheme 2, which began with a Suzuki coupling reaction between 5-bromo-2-hydroxybenzaldehyde (**1.1**) and (4-nonylphenyl)boronic acid to introduce alkyl tails leading to **1.2**. This was next treated with either dibromoethane or *p*-xylene dibromide to produce dimeric products **1.3a** and **1.3b**, respectively, with different linker lengths. These compounds were next subjected to aldehyde reduction to alcohols (**1.4a−b**, shown in the Supporting Information), bromination to produce **1.5a−b**, and then treatment with dipicolylamine to afford compounds **1.6a−b** containing two DPA binding groups. The last step involved zinc chelation, which yielded the desired lipids of type **1** bearing two ZnDPA units.

**Evaluation of Hydrophobic Dye Release from ATP-Responsive Liposomes.** Following lipid switch synthesis, we first employed fluorescence-based dye leakage assays to evaluate the efficacy of these compounds for triggering cargo release when incorporated into liposomes and subjected to different phosphorylated metabolites. Hydrophobic drugs generally benefit from inclusion within nanocarriers to improve pharmacokinetic properties and minimize off-target effects.[54] As a mimic of these drugs, we began by conducting hydrophobic dye release assays using the dye Nile red (NR), which fluoresces when solubilized within membrane bilayers[55] but for which fluorescence is diminished following release into aqueous media.[56] Thus, NR can not only mimic common hydrophobic drug cargo but also provide signal transduction for tracking release. We began by incorporating **1a** at different percentages ranging from 0−20% within liposomes otherwise composed of phosphatidylcholine (PC, mixed isomers from egg) as a traditional bilayer-forming lipid. These unilamellar liposomes were prepared using standard thin-film hydration techniques including film formation, hydration, and freeze/thaw cycling as well as extrusion through a 200 nm membrane. The formation of stable liposomes was verified by dynamic light scattering (DLS) based on average particle sizes (vide infra). NR encapsulation efficiencies were determined using UV−Vis spectroscopy by constructing a NR calibration curve (Figure S1), resulting in (29.30 ± 3.43) and (21.23 ± 3.85)% for PC liposomes containing 0 and 10% **1a**, respectively.

A range of phosphate-containing metabolites were first screened, including inorganic phosphate (Pi), inorganic pyrophosphate (PPi), ATP, adenosine diphosphate (ADP),



https://doi.org/10.1021/jacs.2c00191
J. Am. Chem. Soc. 2022, 144, 3746−3756

adenosine monophosphate (AMP), D-fructose-6-phosphate (FP), and D-fructose-1,6-bisphosphate (FBP). In these experiments, we initially determined that liposomes containing 20% of **1a** showed release only upon ATP and ADP addition among those guests, with slightly greater release in the presence of ATP (Figure 1A). Control PC liposomes did not show any background release. The observed selectivity of **1a** liposomes, ATP > ADP > AMP, could be attributed to the extent of negative charge in these guests.[57] The variation between ATP and ADP treatment led us to hypothesize that ATP/ADP selectivity could be fine-tuned by adjusting the percentage of lipid switch incorporation within liposomes. Specifically, by decreasing the percentage of **1a**, we expected that selectivity for ATP could be enhanced. To this end, we prepared liposomes containing 5 or 10% **1a** and screened them for NR release by phosphorylated metabolites. In line with our hypothesis, only ATP treatment induced a significant amount of dye leakage among these analytes.

Having shown that **1a** liposomes effectively respond to ATP, we next screened NR release upon treatment with additional triphosphate-containing biomolecules including inorganic triphosphate (TPi) and the other nucleotide triphosphates (cytidine (CTP), guanidine (GTP), and uridine (UTP) triphosphate), which are structurally similar metabolites[58] that are also upregulated in tumor cells compared to normal cells,[59] as well as inositol-1,4,5-trisphosphate ($IP_3$), a key signaling molecule that releases calcium stores.[60] As shown in Figure 1B, 10% **1a** liposomes showed release upon treatment with either GTP or UTP. We were somewhat surprised to observe that CTP did not yield any release due to the similarity in structures among nucleotide triphosphates. However, among these, CTP is known to be a weaker electron donor due to the presence of the pyrimidone functionality, which may negate release in this case.[61] Once again, we lowered the **1a** percentage within liposomes to determine if this would enhance selectivity. Accordingly, liposomes containing 5% **1a** exhibited selective NR-driven release by ATP over all other nucleotide triphosphates. These results indicate that designer lipid switch **1a** is effective for selective ATP-triggered liposome release over a range of similar phosphorylated metabolites and that selectivity can be fine-tuned by incorporating different percentages of lipid switches within liposomes. Furthermore, ATP provides a particularly exciting target for metabolite-responsive liposome design due to its important biological roles and upregulation in diseased cells.

A more detailed understanding of ATP-driven NR release from **1a** liposomes is showcased by the titration results in Figure 1C. Here, 2 mM PC liposomes doped with 0, 3, 5, 10, or 20% **1a** were titrated with ATP with fluorescence readings after each addition. The resulting titration curves showed dose-dependent decreases in NR fluorescence as a function of **1a** percentage with PC controls showing no nonspecific release upon ATP treatment. Cargo release proceeded rapidly; when treating 10 or 20% **1a** liposomes with 0.5 mM ATP, release reached a plateau within 3 min after ATP addition (Figure S2). We also conducted release experiments using lower concentrations of liposomes, which led to diminished but still effective release (Supporting Information and Figure S3), suggesting that leakage is somewhat but not entirely driven by liposome fusion. Similar NR release experiments were carried out with compound **1b** (Figure S4A,B). For simple phosphates, 20% **1b** liposomes showed release for both ATP and ADP. However, when the percentage of this compound was decreased to 10%, **1b** liposomes could effectively distinguish between ATP and ADP, although with interference from GTP and slightly from UTP. From the titration profile in Figure S4C, 20 and 10% **1b** liposomes functioned similarly to **1a** liposomes, with ∼50 and ∼40% release for 20 and 10% **1b** incorporation, respectively. Interestingly, when we reduced **1b** incorporation to 5% of the liposome composition, ATP-driven release was almost completely abolished. This result indicates that the cavity present in compound **1a** with an ethyl linker provides an improved fit for ATP binding compared to **1b** (*p*-xylene tether). As a result, liposomes with lower (5%) **1a** incorporation remain effective toward ATP-triggered release. The NR release kinetics of liposomes containing **1b** were also evaluated (Figure S5), which similarly showed that release reached a plateau within 3 min after treating 10 or 20% **1b** liposomes with 0.5 mM ATP. To investigate our proposed conformational change upon **1a**–ATP binding (Scheme 1), diffusion ordered spectroscopy (DOSY) experiments were conducted in solution before and after the addition of ATP (Figure S6). We observed a decrease in diffusion coefficient, from $(1.0793 \pm 0.043) \times 10^{-6}$ $cm^2/s$ for **1a** and $(1.142 \pm 0.018) \times 10^{-6}$ $cm^2/s$ for ATP to $(0.987 \pm 0.098) \times 10^{-6}$ $cm^2/s$ for **1a**–ATP. This result is in accordance with our model by indicating an increase in hydrodynamic radius per lipid molecule upon ATP binding. However, it should be noted that this experiment is performed in solution and thus may not represent how **1a** behaves within the densely packed membrane environment.

**Analysis of Liposome Morphology Changes Driven by ATP.** Triggered release is often accompanied by changes in liposome size and morphology, particularly when processes such as fusion or alterations to lipid self-assembly are involved. Therefore, we next probed potential changes in particle sizes through DLS experiments before and after triggered release. Here, PC liposomes containing 0, 5, 10, or 20% **1a** were subjected to DLS analysis with and without ATP treatment. As can be seen in Figure 2A (gray bars, raw distribution curves in Figure S7), all samples showed uniform particle sizes with expected diameters (∼140 nm) pre-ATP treatment, indicating that stable liposomes were formed with up to at least 20% **1a** incorporation. Upon treatment with 0.5 mM ATP, PC-only liposomes did not show any size change that could result from nonspecific interactions. After ATP addition, however, all liposome samples containing **1a** showed size increases, and the average particle sizes post-ATP correlated with the percentage of **1a** included within the formulation (red bars, Figure 2A). Similar changes in particle sizes were observed for PC/**1b** liposomes (Figure S8). The previously described NR release results indicate that the selectivities of liposomes containing **1a**/**1b** toward ATP over ADP can be fine-tuned by adjusting percent incorporation. These data were further supported through DLS experiments. As shown in Figure S9, uniform size particles were observed for 10% **1a**/**1b** liposomes after ADP treatment, indicating that ADP did not induce significant morphology changes in these cases, in contrast to the dramatic changes observed upon ATP addition.

These results were further supported by electron microscopy (EM) experiments. PC liposomes after ATP addition did not show any change via transmission EM (TEM) imaging using a negative staining technique (Figure S10). The morphology of **1a**/PC liposomes could not survive the negative stain treatment, which is likely due to the charge present on the membrane surface. As a result, we instead explored cryo-EM


https://doi.org/10.1021/jacs.2c00191
J. Am. Chem. Soc. 2022, 144, 3746−3756

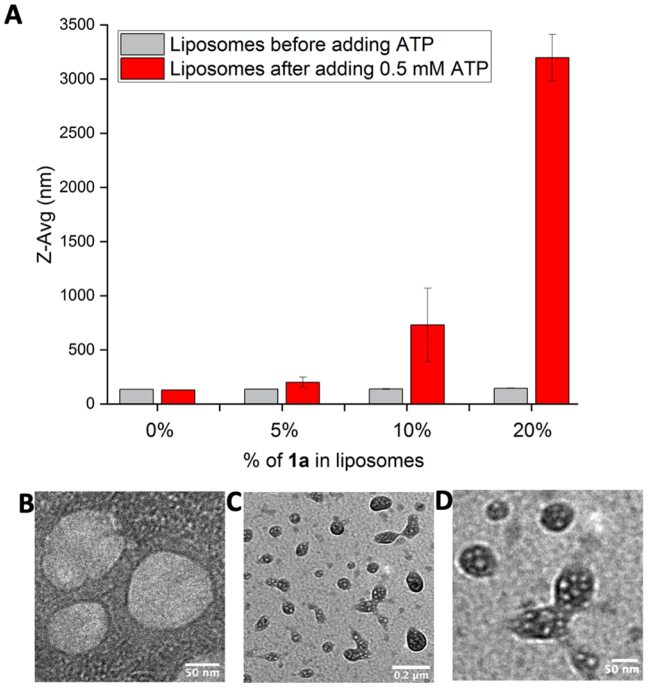


**Figure 2.** (A) DLS analysis of PC-based liposomes containing different percentages of **1a** encapsulating NR before and after ATP treatment. All samples showed uniformly sized particles pre-ATP addition. Increases in particle size were observed for liposomes containing **1a**, and the extent of increase correlated with the percentages of **1a** incorporated. Error bars indicate standard errors from at least three studies. (B) Cryo-EM image of 10% **1a**/PC liposomes before ATP addition showing unilamellar vesicles with expected diameters (scale bar, 50 nm). (C) Cryo-EM image of 10% **1a**/PC liposomes after ATP addition, which instead showed complex multilamellar structures (scale bar, 200 nm). (D) Enlarged image from (C) showing detailed structures of aggregates (scale bar, 50 nm).

imaging, which verified the formation of stable unilamellar 10% **1a**/PC liposomes pre-ATP treatment (Figure 2B). Cryo-EM images for 10% liposomes after 1 min of ATP incubation showed drastic morphology changes (Figures 2C,D), in which the original uniformly sized liposomes were replaced by multivesicular aggregates. In these experiments, cryo-EM images were obtained shortly after ATP addition since prolonged incubation that yielded more complete liposome decomposition made it difficult to obtain images. For this reason, the sizes of lipid nanoparticles in post-ATP images are not as large as the DLS results from more prolonged treatment. We additionally implemented fluorescence microscopy to probe the formation of larger aggregates, which yielded the added benefit of enabling tracking over time. In this experiment, PC liposomes containing 0 or 10% **1a** were labeled with 0.08% rhodamine L-$\alpha$-phosphatidylethanolamine (Rd-PE) and subjected to confocal fluorescence microscopy monitoring over time before and after ATP treatment. As can be seen in the time-course video (Video S1) and the captured images in Figure S11, while both liposomes initially showed very faint fluorescence (original liposome size below microscope resolution), only 10% **1a** liposomes generated highly fluorescent aggregates in the 2−3 $\mu$m size range within 5 min after ATP treatment. Collectively, these results demonstrate changes in the physical properties of liposomes caused by the addition of ATP, for which multiple plausible explanations exist. One possible reason for the size increases of lipid particles involves fusion of liposomes induced by defects in membrane packing. Additionally, changes in lipid structure could induce reorganization of lipids into alternate assemblies such as the inverted hexagonal phase.

We next pondered whether NR release might be reversible. To test this, an ATPase enzyme was used to deplete ATP through hydrolysis into ADP and free phosphate ion. After adding ATP into 10 or 20% **1a** liposomes to trigger content release, the ATPase was added and NR fluorescence was tracked over time. As shown in Figure S12A, addition of the enzyme to 10% liposomes post-ATP treatment completely restored NR fluorescence, and the NR precipitate observed after ATP treatment was redissolved (Figure S12B). DLS experiments following ATPase addition also revealed uniformly sized particles that were identical to the initial liposomes (Figure S12C,D). Interestingly, when the same experiments were conducted using 20% **1a** liposomes, only partial restoration of NR fluorescence (Figure S13A) and particle sizes (Figure S13B−D) was seen. These reversibility results indicate that when lipid **1a** is incorporated at a low percentage (10%), ATP treatment results in mild membrane reorganization that can be reversed when ATP in the system is consumed. However, when **1a** is incorporated at a higher percentage (i.e., 20%), more significant changes in membrane packing likely occur that could lead to liposome fusion, resulting in irreversible release. These results also match our ATP/ADP selectivity results, in which we observed that decreasing **1a** incorporation from 20 to 10% resulted in selectivity for ATP over ADP and other phosphates (Figure 1). This is important to note since ADP produced by ATP hydrolysis could still trigger content release from 20% **1a** liposomes but not from 10% **1a** liposomes. The reversibility data suggest that liposome fusion may be the cause for the reduced ATP specificity observed at 20% **1a**. The ability to manipulate and reverse liposomal self-assembly properties is an exciting result that could be relevant in the context of research investigating the origin of life and mimicking de novo membrane synthesis.[62]

**Assessment of Polar Cargo Triggered Release from ATP-Responsive Liposomes.** Benefitting from their unique bilayer structure, liposomes are also capable of encapsulating and delivering hydrophilic cargo. The release of polar contents from liposomes is also critical, particularly due to rapid recent advances in RNA therapies.[63] Therefore, we next studied the ATP-driven triggering of hydrophilic content release from PC liposomes containing **1a**/**1b**. For these investigations, we employed a calcein dye release assay in which calcein fluorescence is initially quenched at high dye concentrations within liposomes but is then restored upon release that culminates in dilution.[64] Since calcein is nonspecifically encapsulated within liposome interiors during preparation, size-exclusion chromatography (SEC) was performed after extrusion to remove the non-encapsulated dye. The formation of these calcein-encapsulated liposomes was again supported by DLS (Figure S14). The results of this assay were calibrated through treatment with Triton X-100 detergent at the end of each titration to induce complete release. Data are reported as a percentage of the fluorescence intensity induced by Triton X-100 to show the percentage of total release and account for variations in dye inclusion among liposome samples.

To evaluate ATP-responsive properties, we prepared calcein-encapsulated liposomes with 10% **1a** or **1b** in PC as well as control liposomes composed entirely of PC. Calcein


https://doi.org/10.1021/jacs.2c00191
J. Am. Chem. Soc. 2022, 144, 3746−3756

encapsulation efficiency was also determined for 0 and 10% **1a** liposomes[11] and calculated to be (2.16 ± 0.81) and (1.65 ± 0.55)%, respectively. Polar dye encapsulation is typically low since these molecules are randomly trapped during the formation of liposomes.[65] As shown in the kinetic curves in Figure 3 and Figure S15, PC liposomes containing 10% **1a**

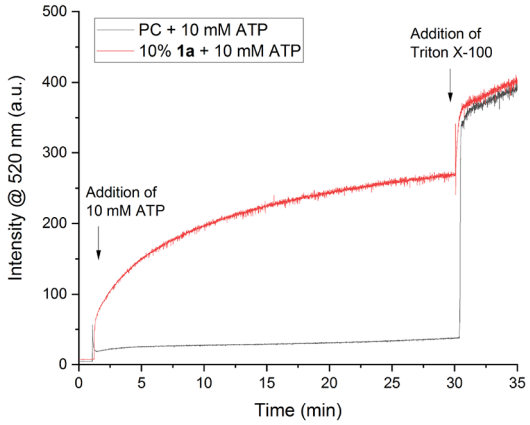


**Figure 3.** Kinetic calcein release curves for PC and 10% **1a**/PC liposomes. Minimal increase in fluorescence intensity was observed for PC liposomes upon treatment with 10 mM ATP. After adding ATP to 10% **1a**/PC liposomes, significant increases in fluorescence were detected. Release was observed to be close to completion within 30 min. Triton X-100 detergent was added after fluorescence increases reached a plateau to induce 100% release and to calibrate this assay. One representative plot of at least three unique experiments is shown.

promoted ∼70% calcein dye release within 30 min upon treatment with 10 mM ATP, while PC control liposomes lacking a lipid switch showed only minimal background release. Again, PC/**1b** liposomes showed comparable release efficacy (Figure S16). Release studies with diluted 10% **1a**/PC liposomes were also conducted and again suggested that fusion is partly but not fully responsible for cargo release (Supporting Information and Figure S17). The potential reversibility of the calcein release assay was also studied, but in this case, ATPase treatment did not affect the kinetic release curve (Figure S18), indicating that the hydrophilic content leakage is an irreversible process as expected. Collectively, our results indicate that lipid switches **1a**−**b** are effective for controlled release of both hydrophobic and hydrophilic cargo release triggered by ATP.

**Evaluation of Binding Interactions between ATP and Free Lipid 1a or 1a Liposomes.** To validate that our lipid switches are effective at binding ATP, the molecular recognition properties of **1a** were next analyzed. First, $^{31}$P NMR titration experiments were carried out to probe for spectral changes resulting from ATP binding.[66] To do so, **1a** was dissolved in $d_6$-DMSO in an NMR tube, which was subjected to titration with a solution of ATP in $D_2O$, with spectra recorded after each aliquot was added. After adding 1 mM ATP (traces A and B, Figure S19), an immediate shift in all three $^{31}$P chemical shifts occurred, indicating the formation of binding interactions between **1a** and ATP. The greatest magnitude in shift change was observed for $P_\alpha$ and $P_\beta$, suggesting that these are closer in proximity to the binding domain. UV−Vis titration experiments were also conducted to further probe binding. When compound **1a** in DMSO was titrated with ATP in $H_2O$, a decrease in absorbance along with a shift in $\lambda_{max}$ was observed, further supporting direct **1a**−ATP binding (Figure S20). Attempts were made to eliminate ATP background absorbance by simultaneously titrating it into a separate reference cell, but this was complicated by the shifting of the host signal upon ATP binding (Figure S20A). Within a liposome environment, binding interactions between **1a** and ATP were evaluated by measuring zeta potential (ZP) values as an efficient means for analyzing changes in surface charge. To do so, liposomes including 0, 5, or 10% of **1a** doped into PC were prepared, and ZP values were measured before and after ATP treatment (Figure S21). Here, 100% PC liposomes initially showed slight negative charge, which is in agreement with the literature[67] and did not change substantially upon ATP incubation. For **1a** liposomes, due to the presence of ZnDPA units within the lipid, initial liposomes were positively charged, and the degree of positive charge correlated with the percentage of **1a** present. After adding ATP, dramatic decreases in positive charge were detected, indicating that ATP is interacting with **1a** and counteracting the positive charge of the ZnDPA units of **1a**.

**Evaluation of Alternative Lipid Switch Structures.** Since we hypothesize that precise structural features are required to control conformational changes, our release results led us to design and synthesize multiple alternative lipid switches bearing different linkers and lipid chains (compounds **1c**−**d** and **2**; Figure 4) to determine effects on activity.

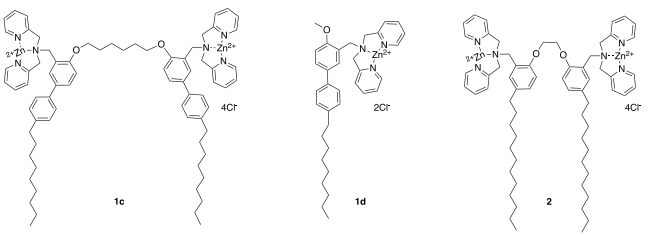


**Figure 4.** Structures of alternative lipid switches designed to probe structural effects on activity. Compared to **1a**, **1c** bears a longer and more flexible hexyl linker. Compound **1d** contains only one ZnDPA binding unit. The rigidities of the lipid tails of **1a** were diminished by switching benzene rings to more flexible hydrocarbons in lipid switch **2**.

Compared to **1a**, **1c** includes a longer and more flexible hexyl linker in between the two ZnDPA units, which was expected to diminish binding and release by increasing the cavity size and flexibility. Analogue **1d** only contains one ZnDPA binding site. If we assume that our lipid switches will be evenly distributed within liposomes otherwise composed of PC, incorporating twice the percentage of **1d** compared to **1a** essentially mimics the longest and most flexible linker that is possible between ZnDPA units. Other than varying the linkers, compound **2** was instead modified within its lipid tails, in which we removed one aromatic ring (rigid) and replaced it with a more flexible C12 alkyl tail. The synthetic routes for these modified compounds are outlined in Schemes S1−S3, which utilized similar strategies as were described for **1a** and **1b**.

NR release efficacy and selectivity were next screened using PC liposomes doped with 10 or 20% **1c**−**d**/**2**. While these lipids generally remained effective for ATP-mediated release, as was expected, they were overall less responsive, which was in line with our hypothesis. Compared to 10% **1a** liposomes, which exhibited release by ATP, GTP, and UTP, 10% **1c**


https://doi.org/10.1021/jacs.2c00191
J. Am. Chem. Soc. 2022, 144, 3746−3756

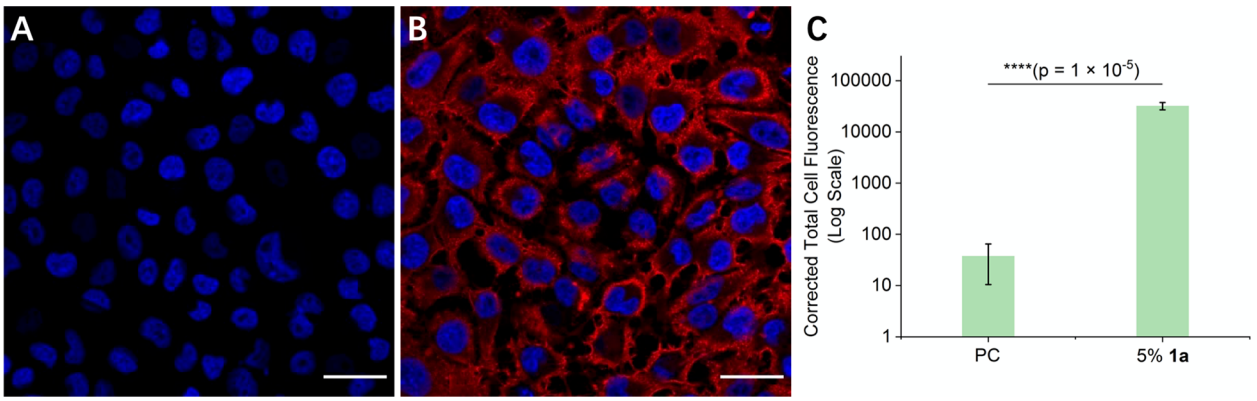


**Figure 5.** Fluorescence images of A375 cells treated with PC/Rd-PE liposomes (A) or 5% **1a**/PC/Rd-PE liposomes (B) for 30 min. The presence of **1a** increases cellular uptake of liposomes while PC liposomes without **1a** showed minimal cellular infiltration. Blue, DAPI; red, Rd-PE. Scale bars, 30 $\mu$m. (C) Quantified corrected total cell fluorescence via ImageJ. Statistical analysis ($t$ test) indicates that there is a significant increase ($p = 1.7 \times 10^{-5}$) in uptake when 5% **1a** is present in PC liposomes. $N = 4$. Error bars indicate standard deviation from the mean.

liposomes exhibited reduced activity and responded only to ATP and GTP (Figure S22A,B). Similar results were observed for 20% **1d** liposomes, which contain the same number of ZnDPA binding sites on liposome surfaces as would 10% of **1a−c** (Figure S23A,B). Further decreasing **1d** incorporation to 10% completely abrogated release. The ATP-responsive properties of each compound were thoroughly evaluated by expanded NR release titrations for PC liposomes containing 5−20% of **1c−d/2** (Figures S22C, S23C, and S24C). While 10% **1a** and **1b** liposomes showed comparable ATP release properties, 10% **1c** liposomes exhibited much slower kinetics (Figure S22C), which were similar to 20% **1d** liposomes (Figure S23C). Upon altering lipid chains, PC liposomes containing 10% **2**, which simply differs from **1a** via more flexible lipid chains, only responded to ATP among all the phosphorylated guest molecules we tested (Figure S24A,B). However, while 20% **1a−c** liposomes showed very fast release kinetics upon ATP binding, slightly slower release was observed for 20% **2** liposomes. In addition, 10% **2** liposomes showed an obvious longer induction period, indicating that rigidity within the tail also affects ATP binding/triggered release properties. Although $\pi-\pi$ stacking interactions contribute to certain ATP sensors,[68] we do not expect this to be a significant effect in our compounds, considering that aromatic tails are expected to be far away from the binding sites and buried in the hydrophobic membrane core, making them inaccessible to water-soluble ATP. Reductions in conformational changes induced by ATP binding provide a more reasonable explanation for the diminished release properties when switching rigid aromatic tails to more flexible aliphatic tails. NR release results using all lipid switches studied herein are summarized in Table S1. DLS and calcein release experiments yielded similar conclusions regarding the ATP-responsive properties of **1c−d/2** (Supporting Information and Figures S22D, S23D, S24D, and S25−S28).

These results indicate that increasing flexibility in both the linker between ZnDPAs and in the lipid chains indeed reduced liposome release via these lipid switches induced by ATP and the other metabolites we tested. Specifically, conversion from the ethyl linker of **1a** to the hexyl linker of **1c** led to loss of activity, and no further reduction was observed using double the concentration of **1d**, which contains only one ZnDPA domain. This shows that maintaining a proper cavity size is critical for effective molecular recognition events and/or conformational changes that drive release. These results support our hypothesis that controlling the spacing of binding groups within lipid switches is critical for optimizing conformational changes that drive release. Furthermore, diminishing general activity toward phosphorylated biomolecules provides an avenue for achieving greater selectivity toward ATP, since activities toward other metabolites can be decreased to a greater extent.

**Cellular Delivery Studies Employing Modulation of ATP Abundance.** After demonstrating the successful design of stimuli-responsive liposomes that selectively release contents in the presence of ATP, we next conducted fluorescence microscopy experiments to determine whether **1a** liposomes are a viable means to deliver encapsulated molecules to cells. Additionally, we determined whether cargo release is controlled by ATP levels. For these experiments, we employed PC-based liposomes containing 5% **1a**, a percentage determined to exhibit ATP-selectivity in release studies, which were also doped with 0.08% Rd-PE. This fluorescently tagged lipid enables facile detection of liposome uptake using optical microscopy techniques. Liposomes were incubated with A375 melanoma cells for 30 min at 37 °C in a $CO_2$ environment, washed to remove unbound liposomes, labeled with DAPI (cell nuclei), fixed, and mounted on glass slides for imaging. In initial experiments, cells treated with 5% **1a** liposomes (Figure 5B) were compared to those subjected to PC control liposomes (Figure 5A), which showcased a drastic enhancement in Rd fluorescence resulting from cellular delivery. Corrected total cell fluorescence (CTCF) values showed a ∼1000-fold increase in cell delivery driven by **1a** (Figure 5C). These results indicate that **1a** is effective for driving liposomal cell entry. Cell viability in the presence of ATP-responsive liposomes was also measured via an MTS assay using 5% **1a**/PC liposomes, with results showing that **1a** liposomes do not cause cytotoxicity (Figure S29).

We next worked to ascertain the dependence of cellular delivery specifically on ATP abundance, in which drugs were employed that modulate intracellular ATP biosynthesis. Specifically, combined treatment with antimycin A (AA) and 2-deoxy-D-glucose (DG) was first conducted to inhibit mETC complex III and glycolysis, respectively, which decreases intracellular ATP levels.[69] Treatment with 5-aminoimidazole-4-carboxamide-1-$\beta$-riboside (AICAR), on the other hand, increases intracellular ATP concentrations by activating


https://doi.org/10.1021/jacs.2c00191
J. Am. Chem. Soc. 2022, 144, 3746−3756

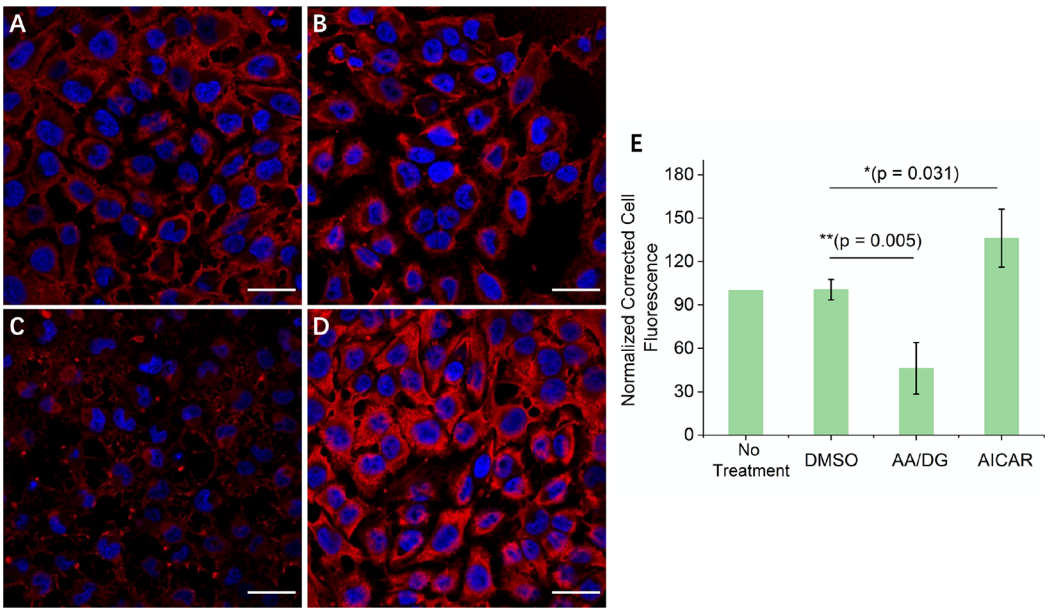


**Figure 6.** Fluorescence images of control cells (A), control cells including diluted DMSO (B), cells treated with AA/DG (C), or AICAR (D) followed by the addition of PC/**1a** (5%)/Rd-PE liposomes for 30 min. Intracellular ATP modifications affect cellular uptake of vesicles containing lipid **1a**. Upregulating intracellular ATP increased liposome uptake, while downregulating ATP level decreased uptake. Blue, DAPI; red, Rd-PE. Scale bar, 30 $\mu$m. (E) CTCF values normalized to the untreated cell condition. One-way ANOVA ($p$ = 0.0003) with post hoc Tukey test showed a significant decrease in uptake when cells were pretreated with AA/DG and a significant increase in uptake when cells were pretreated with AICAR. $N$ = 3−4. Error bars show the standard deviation from the mean.

AMPK.[70] Intracellular ATP concentrations upon inhibitor treatment were quantified using a commercially available luminescent ATP detection assay kit (Figure S30A). Modulation of ATP concentrations led to profound effects on cellular delivery. Treatment with AA/DG to diminish intracellular ATP resulted in a significant decrease in cellular uptake (Figure 6C) compared to untreated cells (Figure 6A). Conversely, increase of ATP abundance using AICAR instead culminated in significantly increased uptake (Figure 6D). A control containing diluted DMSO (Figure 6B) was also run since AA was dissolved in DMSO. In all cases, fluorescence intensities were quantified as indicated in Figure 6E. The data resulting from pharmacological ATP modification indicate that cellular delivery changes do not merely arise from different degrees of endocytosis. While cells with downregulated ATP resulting from treatment with AA/DG did yield some labeling, the minimal amount of delivery observed in these experiments may potentially result from the ability of ZnDPA groups to interact with cell surfaces by binding to anionic phospholipids.[51]

Overall, these results culminate in the conclusion that cellular delivery of **1a** liposomes is indeed driven by ATP and correlates with ATP concentrations. One potential explanation for this result involves literature evidence that intracellular ATP is released from cells through both active and passive pathways, especially in the case of dying or damaged cells.[71,72] Furthermore, **1a** liposomes can potentially interact with cell membranes and induce transient pore formation, which is a known mechanism by which cationic peptides and DNA/lipoplexes can induce intracellular ATP leakage.[73] To explore these possibilities, we measured extracellular ATP abundance and found that sub-micromolar levels were present in the cellular environment (Figure S30B). Since the results shown in Figure 1C indicate that release from liposomes containing **1a** requires significantly higher ATP concentrations, we therefore conclude that these low extracellular ATP levels are unlikely to play an important role in cellular delivery. Furthermore, we determined that **1a** liposomes do not promote ATP cellular leakage. We instead propose that the higher levels of ATP contained within late endosomes may constitute the main source of ATP that drives liposome release. The notion that intracellular ATP is key for cargo release is supported by the results obtained with AA/DG and AICAR (Figure 6E). In accordance with these results, we propose that intracellular ATP compromises **1a** liposomes following their uptake into cells, resulting in their decomposition and release of contents.

## CONCLUSIONS

We successfully developed small molecule responsive liposomes that exhibit selectivity for ATP among a variety of phosphorylated metabolites using synthetic lipid switches that are driven by molecular recognition principles. This represents a new paradigm for controlled liposome release by exploiting critical and complex small molecule metabolites as triggers. Liposome delivery was achieved through the engineering of lipid structures to undergo binding interactions with specific guest molecules in a manner that modulates lipid self-assembly properties. Specifically, two phosphate-binding ZnDPA units were introduced within the rigid lipid scaffold of **1a**, such that ATP binding induces a conformational change within the lipid structure. This molecular arrangement promotes non-bilayer properties and disrupts membrane integrity to ultimately induce encapsulated cargo release. Our data show that **1a** is highly effective as a lipid switch for driving ATP-responsive liposome cargo release. Furthermore, our results demonstrate that release properties can be fine-tuned to tailor selectivity toward ATP by modulating the percentage of **1a** within liposomes. Systematic evaluation of ATP binding properties, release of hydrophobic and hydrophilic cargo, and lipid nanoparticle characteristics collectively showed that selective


https://doi.org/10.1021/jacs.2c00191
J. Am. Chem. Soc. 2022, 144, 3746−3756

ATP-mediated liposome release was achieved through the modulation of lipid self-assembly properties via ATP/lipid switch binding. By evaluating multiple alternative lipid switch structures with varying flexibilities both in the linker between the ZnDPA units and within the lipid tails (**1a−d/2**), we showed that structural fit is critical for optimizing release properties. Finally, cellular fluorescence microscopy experiments demonstrated that **1a** liposomes are effective for cellular uptake controlled by intracellular ATP levels. This new direction offers an exciting avenue for enhancing control over liposome release by harnessing important biomolecules that are overabundant in disease. We envision that other aberrantly expressed biomolecules can act as targets for liposomal triggered release by designing complementary lipid switches using similar design strategies.

## ■ ASSOCIATED CONTENT

### Supporting Information

The Supporting Information is available free of charge at https://pubs.acs.org/doi/10.1021/jacs.2c00191.

Supplemental text; experimental procedures; supplemental figures; characterization of synthetic compounds (PDF)

Videos for liposomes morphology changes after adding ATP using fluorescence microscope (MP4)

## ■ AUTHOR INFORMATION


### Corresponding Author

**Michael D. Best** − *Department of Chemistry, University of Tennessee, Knoxville, Tennessee 37996, United States;* orcid.org/0000-0001-8737-5910; Email: mdbest@utk.edu

### Authors

**Jinchao Lou** − *Department of Chemistry, University of Tennessee, Knoxville, Tennessee 37996, United States;* orcid.org/0000-0001-5064-761X

**Jennifer A. Schuster** − *Department of Biochemistry & Cellular and Molecular Biology, University of Tennessee, Knoxville, Tennessee 37996, United States*

**Francisco N. Barrera** − *Department of Biochemistry & Cellular and Molecular Biology, University of Tennessee, Knoxville, Tennessee 37996, United States;* orcid.org/0000-0002-5200-7891

Complete contact information is available at: https://pubs.acs.org/10.1021/jacs.2c00191


### Author Contributions

The manuscript was written through contributions of all authors. All authors have given approval to the final version of the manuscript.

### Notes

The authors declare no competing financial interest.

## ■ ACKNOWLEDGMENTS

This material is based upon work supported by the National Science Foundation under grant DMR-1807689 (to M.D.B.) and by National Institutes of Health grant R35GM140846 (to F.N.B.). We would like acknowledge Dr. Trevor McQueen of Neptune Fluid Flow Systems LLC (neptuneffs@gmail.com) for his contribution to helping us vitrify this challenging specimen, Dr. John Dunlap for assistance with TEM, Jaydeep Kolape for assistance with fluorescence microscopy, and Mahshid Mokhtarnejad and Dr. Bamin Khomami for assistance with DLS experiments.

## ■ REFERENCES


(1) Pattni, B. S.; Chupin, V. V.; Torchilin, V. P. New developments in liposomal drug delivery. *Chem. Rev.* **2015**, *115*, 10938−10966.

(2) Allen, T. M.; Cullis, P. R. Liposomal drug delivery systems: From concept to clinical applications. *Adv. Drug Del. Rev.* **2013**, *65*, 36−48.

(3) Jhaveri, A.; Deshpande, P.; Torchilin, V. Stimuli-sensitive nanopreparations for combination cancer therapy. *J. Controlled Release* **2014**, *190*, 352−370.

(4) Lasic, D. D.; Needham, D. The "Stealth" liposome: A prototypical biomaterial. *Chem. Rev.* **1995**, *95*, 2601−2628.

(5) Gao, H.; Zhang, Q.; Yu, Z.; He, Q. Cell-penetrating peptide-based intelligent liposomal systems for enhanced drug delivery. *Curr. Pharm. Biotechnol.* **2014**, *15*, 210−219.

(6) Manjappa, A. S.; Chaudhari, K. R.; Venkataraju, M. P.; Dantuluri, P.; Nanda, B.; Sidda, C.; Sawant, K. K.; Murthy, R. S. R. Antibody derivatization and conjugation strategies: Application in preparation of stealth immunoliposome to target chemotherapeutics to tumor. *J. Controlled Release* **2011**, *150*, 2−22.

(7) Mura, S.; Nicolas, J.; Couvreur, P. Stimuli-responsive nanocarriers for drug delivery. *Nat. Mater.* **2013**, *12*, 991−1003.

(8) Alam, S.; Mattern-Schain, S. I.; Best, M. D., Targeting and triggered release using lipid-based supramolecular assemblies as medicinal nanocarriers. In *Comprehensive Supramolecular Chemistry Volume 2*, Atwood, J. L., Ed. Elsevier: 2017; Vol. *5*, pp. 329−364, DOI: 10.1016/B978-0-12-409547-2.12540-5.

(9) Paliwal, S. R.; Paliwal, R.; Vyas, S. P. A review of mechanistic insight and application of pH-sensitive liposomes in drug delivery. *Drug Delivery* **2015**, *22*, 231−242.

(10) Ferreira, D. D. S.; Lopes, S. C. D. A.; Franco, M. S.; Oliveira, M. C. pH-sensitive liposomes for drug delivery in cancer treatment. *Ther. Delivery* **2013**, *4*, 1099−1123.

(11) Ong, W.; Yang, Y.; Cruciano, A. C.; McCarley, R. L. Redox-triggered contents release from liposomes. *J. Am. Chem. Soc.* **2008**, *130*, 14739−14744.

(12) Wang, Z.; Ling, L.; Du, Y.; Yao, C.; Li, X. Reduction responsive liposomes based on paclitaxel-ss-lysophospholipid with high drug loading for intracellular delivery. *Int. J. Pharm.* **2019**, *564*, 244−255.

(13) Lou, J.; Best, M. D. Reactive oxygen species-responsive liposomes via boronate-caged phosphatidylethanolamine. *Bioconjugate Chem.* **2020**, *31*, 2220−2230.

(14) Hu, Q.; Katti, P. S.; Gu, Z. Enzyme-responsive nanomaterials for controlled drug delivery. *Nanoscale* **2014**, *6*, 12273−12286.

(15) Lou, J.; Best, M. D. A general approach to enzyme-responsive liposomes. *Chem. − Eur. J.* **2020**, *26*, 8597−8607.

(16) Bayer, A. M.; Alam, S.; Mattern-Schain, S. I.; Best, M. D. Triggered liposomal release through a synthetic phosphatidylcholine analogue bearing a photocleavable moiety embedded within the sn-2 acyl chain. *Chem. − Eur. J.* **2014**, *20*, 3350−3357.

(17) Puri, A. Phototriggerable liposomes: current research and future perspectives. *Pharmaceutics* **2014**, *6*, 1−25.

(18) Ta, T.; Porter, T. M. Thermosensitive liposomes for localized delivery and triggered release of chemotherapy. *J. Controlled Release* **2013**, *169*, 112−125.

(19) Kneidl, B.; Peller, M.; Winter, G.; Lindner, L. H.; Hossann, M. Thermosensitive liposomal drug delivery systems: state of the art review. *Int. J. Nanomed.* **2014**, *9*, 4387−4398.

(20) Huang, S.-L. Liposomes in ultrasonic drug and gene delivery. *Adv. Drug Delivery Rev.* **2008**, *60*, 1167−1176.

(21) Webb, B. A.; Chimenti, M.; Jacobson, M. P.; Barber, D. L. Dysregulated pH: A perfect storm for cancer progression. *Nat. Rev. Cancer* **2011**, *11*, 671−677.

(22) Fisher, G. J.; Wang, Z.; Datta, S. C.; Varani, J.; Kang, S.; Voorhees, J. J. Pathophysiology of premature skin aging induced by ultraviolet light. *N. Engl. J. Med.* **1997**, *337*, 1419−1429.
(23) Lou, J.; Carr, A. J.; Watson, A. J.; Mattern-Schain, S. I.; Best, M. D. Calcium-responsive liposomes via a synthetic lipid switch. *Chem. − Eur. J.* **2018**, *24*, 3599−3607.
(24) Sagar, R.; Lou, J.; Watson, A. J.; Best, M. D. Zinc triggered release of encapsulated cargo from liposomes via a synthetic lipid switch. *Bioconjugate Chem.* **2021**, *32*, 2485−2496.
(25) Humphrey, S. J.; James, D. E.; Mann, M. Protein phosphorylation: a major switch mechanism for metabolic regulation. *Trends Endocrinol. Metab.* **2015**, *26*, 676−687.
(26) Wilson, D. F. Oxidative phosphorylation: regulation and role in cellular and tissue metabolism. *J. Physiol.* **2017**, *595*, 7023−7038.
(27) Zimmermann, H. Signalling via ATP in the nervous system. *Trends Neurosci.* **1994**, *17*, 420−426.
(28) El-Moatassim, C.; Dornand, J.; Mani, J.-C. Extracellular ATP and cell signalling. *Biochim. Biophys. Acta, Mol. Cell Res.* **1992**, *1134*, 31−45.
(29) Elston, T.; Wang, H.; Oster, G. Energy transduction in ATP synthase. *Nature* **1998**, *391*, 510−513.
(30) Martin, W. F.; Thauer, R. K. Energy in ancient metabolism. *Cell* **2017**, *168*, 953−955.
(31) Nichols, C. G. KATP channels as molecular sensors of cellular metabolism. *Nature* **2006**, *440*, 470−476.
(32) Ashcroft, S. J. H.; Ashcroft, F. M. Properties and functions of ATP-sensitive K-channels. *Cell. Signalling* **1990**, *2*, 197−214.
(33) Bell, S. P.; Stillman, B. ATP-dependent recognition of eukaryotic origins of DNA replication by a multiprotein complex. *Nature* **1992**, *357*, 128−134.
(34) Vincent, J. A.; Kwong, T. J.; Tsukiyama, T. ATP-dependent chromatin remodeling shapes the DNA replication landscape. *Nat. Struct. Mol. Biol.* **2008**, *15*, 477−484.
(35) Gilbert, S. M.; Oliphant, C. J.; Hassan, S.; Peille, A. L.; Bronsert, P.; Falzoni, S.; Di Virgilio, F.; McNulty, S.; Lara, R. ATP in the tumour microenvironment drives expression of nfP2X7, a key mediator of cancer cell survival. *Oncogene* **2019**, *38*, 194−208.
(36) Zheng, L. M.; Zychlinsky, A.; Liu, C. C.; Ojcius, D. M.; Young, J. D. Extracellular ATP as a trigger for apoptosis or programmed cell death. *J. Cell Biol.* **1991**, *112*, 279−288.
(37) Di Virgilio, F.; Dal Ben, D.; Sarti, A. C.; Giuliani, A. L.; Falzoni, S. The P2X7 receptor in infection and inflammation. *Immunity* **2017**, *47*, 15−31.
(38) Di Virgilio, F.; Sarti, A. C.; Falzoni, S.; De Marchi, E.; Adinolfi, E. Extracellular ATP and P2 purinergic signalling in the tumour microenvironment. *Nat. Rev. Cancer* **2018**, *18*, 601−618.
(39) Sun, W.; Gu, Z. ATP-responsive drug delivery systems. *Expert Opin. Drug. Delivery* **2016**, *13*, 311−314.
(40) He, Q.; Chen, J.; Yan, J.; Cai, S.; Xiong, H.; Liu, Y.; Peng, D.; Mo, M.; Liu, Z. Tumor microenvironment responsive drug delivery systems. *Asian J. Pharm. Sci.* **2020**, *15*, 416−448.
(41) Sameiyan, E.; Bagheri, E.; Dehghani, S.; Ramezani, M.; Alibolandi, M.; Abnous, K.; Taghdisi, S. M. Aptamer-based ATP-responsive delivery systems for cancer diagnosis and treatment. *Acta Biomater.* **2021**, *123*, 110−122.
(42) Chen, W.-H.; Yu, X.; Liao, W.-C.; Sohn, Y. S.; Cecconello, A.; Kozell, A.; Nechushtai, R.; Willner, I. ATP-responsive aptamer-based metal−organic framework nanoparticles (NMOFs) for the controlled release of loads and drugs. *Adv. Funct. Mater.* **2017**, *27*, 1702102.
(43) Liao, W.-C.; Sohn, Y. S.; Riutin, M.; Cecconello, A.; Parak, W. J.; Nechushtai, R.; Willner, I. The application of stimuli-responsive VEGF- and ATP-aptamer-based microcapsules for the controlled release of an anticancer drug, and the selective targeted cytotoxicity toward cancer cells. *Adv. Funct. Mater.* **2016**, *26*, 4262−4273.
(44) Mo, R.; Jiang, T.; Gu, Z. Enhanced anticancer efficacy by ATP-mediated liposomal drug delivery. *Angew. Chem., Int. Ed.* **2014**, *53*, 5815−5820.
(45) van den Brink-van der Laan, E.; Killian, J. A.; de Kruijff, B. Nonbilayer lipids affect peripheral and integral membrane proteins via changes in the lateral pressure profile. *Biochim. Biophys. Acta* **2004**, *1666*, 275−288.
(46) Lou, J.; Best, M. D. Strategies for altering lipid self-assembly to trigger liposome cargo release. *Chem. Phys. Lipids* **2020**, *232*, 104966.
(47) Lou, J.; Zhang, X.; Best, M. D. Lipid switches: Stimuli-responsive liposomes through conformational isomerism driven by molecular recognition. *Chem. − Eur. J.* **2019**, *25*, 20−25.
(48) Mbarek, A.; Moussa, G.; Leblond Chain, J. Pharmaceutical applications of molecular tweezers, clefts and clips. *Molecules* **2019**, *24*, 1803.
(49) Viricel, W.; Mbarek, A.; Leblond, J. Switchable lipids: Conformational change for fast pH-triggered cytoplasmic delivery. *Angew. Chem., Int. Ed.* **2015**, *54*, 12743−12747.
(50) Viricel, W.; Poirier, S.; Mbarek, A.; Derbali, R. M.; Mayer, G.; Leblond, J. Cationic switchable lipids: pH-triggered molecular switch for siRNA delivery. *Nanoscale* **2017**, *9*, 31−36.
(51) Rice, D. R.; Clear, K. J.; Smith, B. D. Imaging and therapeutic applications of zinc(ii)-dipicolylamine molecular probes for anionic biomembranes. *Chem. Commun.* **2016**, *52*, 8787−8801.
(52) Ngo, H. T.; Liu, X.; Jolliffe, K. A. Anion recognition and sensing with Zn (II)−dipicolylamine complexes. *Chem. Soc. Rev.* **2012**, *41*, 4928−4965.
(53) Smith, B. D.; Anslyn, E.; Gokel, G.; Kubik, S.; Wang, B.; Hong, J.-I.; Hargrove, A.; Schmuck, C.; Rotello, D.; Gale, P., *Synthetic receptors for biomolecules: Design principles and applications*. Royal Society of Chemistry: 2015, DOI: 10.1039/9781782622062.
(54) Allen, T. M. Liposomal drug formulations. *Drugs* **1998**, *56*, 747−756.
(55) Greenspan, P.; Mayer, E. P.; Fowler, S. D. Nile red: a selective fluorescent stain for intracellular lipid droplets. *J. Cell. Biol.* **1985**, *100*, 965−973.
(56) Liang, X.; Yue, X.; Dai, Z.; Kikuchi, J.-i. Photoresponsive liposomal nanohybrid cerasomes. *Chem. Commun.* **2011**, *47*, 4751−4753.
(57) Deng, J.; Walther, A. ATP-responsive and ATP-fueled self-assembling systems and materials. *Adv. Mater.* **2020**, *32*, 2002629.
(58) Chen, Z.-P.; Levy, A.; Lightman, S. L. Nucleotides as extracellular signalling molecules. *J. Neuroendocrinol.* **1995**, *7*, 83−96.
(59) Traut, T. W. Physiological concentrations of purines and pyrimidines. *Mol. Cell. Biochem.* **1994**, *140*, 1−22.
(60) Jayaraman, T.; Ondriasova, E.; Ondrias, K.; Harnick, D. J.; Marks, A. R. The inositol 1, 4, 5-trisphosphate receptor is essential for T-cell receptor signaling. *Proc. Natl. Acad. Sci.* **1995**, *92*, 6007−6011.
(61) Jose, D. A.; Mishra, S.; Ghosh, A.; Shrivastav, A.; Mishra, S. K.; Das, A. Colorimetric sensor for ATP in aqueous solution. *Org. Lett.* **2007**, *9*, 1979−1982.
(62) Vance, J. A.; Devaraj, N. K. Membrane mimetic chemistry in artificial cells. *J. Am. Chem. Soc.* **2021**, *143*, 8223−8231.
(63) Miller, A. D. Cationic liposomes for gene therapy. *Angew. Chem., Int. Ed.* **1998**, *37*, 1768−1785.
(64) Allen, T., *Calcein as a tool in liposome methodology*. CRC Press, Boca Raton, Florida: 1984.
(65) Eloy, J. O.; Claro de Souza, M.; Petrilli, R.; Barcellos, J. P. A.; Lee, R. J.; Marchetti, J. M. Liposomes as carriers of hydrophilic small molecule drugs: strategies to enhance encapsulation and delivery. *Colloids Surf., B* **2014**, *123*, 345−363.
(66) Ojida, A.; Park, S.-k.; Mito-Oka, Y.; Hamachi, I. Efficient fluorescent ATP-sensing based on coordination chemistry under aqueous neutral conditions. *Tetrahedron Lett.* **2002**, *43*, 6193−6195.
(67) Fatouros, D. G.; Antimisiaris, S. G. Effect of amphiphilic drugs on the stability and zeta-potential of their liposome formulations: A study with prednisolone, diazepam, and griseofulvin. *J. Colloid Interface Sci.* **2002**, *251*, 271−277.
(68) Farshbaf, S.; Anzenbacher, P. Fluorimetric sensing of ATP in water by an imidazolium hydrazone based sensor. *Chem. Commun.* **2019**, *55*, 1770−1773.
(69) Holmsen, H.; Setkowsky, C. A.; Day, H. J. Effects of antimycin and 2-deoxyglucose on adenine nucleotides in human platelets. Role of metabolic adenosine triphosphate in primary aggregation,

secondary aggregation and shape change of platelets. *Biochem. J.* **1974**, *144*, 385−396.
(70) Ke, R.; Xu, Q.; Li, C.; Luo, L.; Huang, D. Mechanisms of AMPK in the maintenance of ATP balance during energy metabolism. *Cell Biol. Int.* **2018**, *42*, 384−392.
(71) Vultaggio-Poma, V.; Sarti, A. C.; Di Virgilio, F. Extracellular ATP: A feasible target for cancer therapy. *Cell* **2020**, *9*, 2496.
(72) Dosch, M.; Gerber, J.; Jebbawi, F.; Beldi, G. Mechanisms of ATP release by inflammatory cells. *Int. J. Mol. Sci.* **2018**, *19*, 1222.
(73) van der Woude, I.; Visser, H. W.; ter Beest, M. B. A.; Wagenaar, A.; Ruiters, M. H. J.; Engberts, J. B. F. N.; Hoekstra, D. Parameters influencing the introduction of plasmid DNA into cells by the use of synthetic amphiphiles as a carrier system. *Biochim. Biophys. Acta, Biomembr.* **1995**, *1240*, 34−40.



https://doi.org/10.1021/jacs.2c00191
*J. Am. Chem. Soc.* 2022, 144, 3746−3756